ENERGY OF MICROWAVE-EMITTING ELECTRONS AND HARD X-RAY/MICROWAVE SOURCE MODEL IN SOLAR FLARES

NARIAKI NITTA

Tokyo Astronomical Observatory, University of Tokyo, Mitaka, Tokyo, 181 Japan

and

TAKEO KOSUGI*

Laboratory for Astronomy and Solar Physics, NASA Goddard Space Flight Center, Greenbelt, MD 20771, U.S.A.

(Received 16 October, 1985; in revised form 7 March, 1986)

Abstract. We present a new method of estimating the energy of microwave-emitting electrons from the observed rate of increase of the microwave flux relative to the hard X-ray flux measured at various energies during the rising phase of solar flares. A total of 22 flares observed simultaneously in hard X-rays (20–400 keV) and in microwaves (17 GHz) were analyzed in this way and the results are as follows:

(1) The observed energy of X-rays which vary in proportion to the 17 GHz emission concentrates mostly below 100 keV with a median energy of 70 keV. Since the mean energy of electrons emitting 70 keV X-rays is $\lesssim$130 keV or $\lesssim$180 keV, depending on the assumed hard X-ray emission model (thin-target and thick-target, respectively), this photon energy strongly suggests that the 17 GHz emission comes mostly from electrons with an energy of less than a few hundred keV.

(2) Correspondingly, the magnetic field strength in the microwave source is calculated to be 500–1000 G for the thick-target case and 1000–2000 G for the thin-target case. Finally, judging from the values of the source parameters required for the observed microwave fluxes, we conclude that the thick-target model in which precipitating electrons give rise to both X-rays and microwaves is consistent with the observations for at least 16 out of 22 flares examined.

1. Introduction

In solar flares, both the similarity of hard X-ray and microwave time profiles (Crannell *et al.*, 1978; Cornell *et al.*, 1984) and the good correlation of peak fluxes (Kane, 1974; Kai *et al.*, 1985) lead us to consider that the two kinds of emission are due to commonly accelerated electrons, that the sources of two emissions are probably the same or at least not far from each other, and that the energy of microwave-emitting electrons is close to that of electrons responsible for hard X-ray emission in relatively low energies. In this paper we present a new method of estimating the energy range of electrons contributing most effectively to microwaves, and of determining the hard X-ray emission model (thick-target or thin-target) and the microwave source parameters (for example, the magnetic field strength).

The proposed method of estimating the mean energy of microwave-emitting electrons ($\bar{E}_\mu$) is based on the observed rate of increase of the microwave flux relative to the hard X-ray flux at various energies from the onset to the peak of a flare. The hardening of the energy spectrum of energetic electrons, inferred from the hardening of the X-ray

* NAS/NRC Research Associate, on leave from Tokyo Astronomical Observatory.

Solar Physics **105** (1986) 73–85.

spectrum during the rising phase (Kane and Anderson, 1970; Crannell *et al.*, 1978; Kane *et al.*, 1980), causes the difference of the flux increase between microwaves (assumed to be optically thin) and X-rays; the rate of increase of the microwave flux is greater than, almost equal to, or smaller than that of X-rays of energy ε, depending on the condition that $\overline{E_\mu} > \overline{E_X}$, $\overline{E_\mu} \sim \overline{E_X}$, or $\overline{E_\mu} < \overline{E_X}$, respectively, where $\overline{E_X}$ is the mean energy of electrons emitting X-rays of energy ε. Then, we can estimate $\overline{E_\mu}$ from the energy $\tilde{\varepsilon}$ of X-rays which increase at the same rate as microwaves, because $\overline{E_X}$ can be related to $\tilde{\varepsilon}$ if the hard X-ray emission model is known.

The flux increase of microwaves relative to that of hard X-rays depends on both the X-ray emission model (thin-target or thick-target) and the magnetic field strength in the microwave source. For each of the two X-ray emission models, the magnetic field strength in the microwave source is derived from the comparison between the calculated and observed rate of flux increase. Next, we judge which of the two possibilities is more likely, fitting the calculated microwave flux to the observed flux. We consider the model to be likely when the derived value of a parameter such as the length of the microwave source or the ambient ion density in the X-ray source is compatible with the observed value.

Previous works of estimating the magnetic field strength or the energy range of electrons in the microwave source are primarily based on the comparison between the calculated and observed flux at the peak of a flare (e.g., Holt and Cline, 1968; Holt and Ramaty, 1969; Takakura, 1972; Gary, 1985; Kai, 1986). However, it is not possible from this procedure alone to determine both the X-ray emission model and the magnetic field strength in the microwave source.

In the next section, we present the analysis of observed data; the rate of increase of the 17 GHz flux is defined with respect to that of the X-ray counting rates measured at various energies, and the energy $\tilde{\varepsilon}$ of X-rays increasing at the same rate as the 17 GHz flux is obtained. In Section 3, we calculate the energy range of electrons emitting the X-rays of energy $\tilde{\varepsilon}$, and estimate the mean energy of microwave-emitting electrons. In Section 4, we obtain the magnetic field strength for which the rate of increase of the 17 GHz flux relative to the X-ray flux at different energies agrees with the observations and then determine both the hard X-ray emission model and the microwave source model. In Section 5, we summarize and discuss the results.

2. Observations and Analysis

During the period of February 1981 to August 1982, more than 60 flares were observed simultaneously by the Hard X-Ray Monitor Spectrometer on Hinotori (HXM, see Ohki *et al.*, 1982; Nitta, 1984) covering the energy range from 30 (or 15) to 400 keV in 7 channels and by the 17 GHz polarimeter at Nobeyama. We have selected 22 of these flares with the criteria that there are enough excess counting rates in the HXM channel 4 (67–107 keV) at the peak of the event, and that both the hard X-ray and 17 GHz data are available from the beginning. These 22 flares, though restricted to relatively intense ones, cover rather wide ranges of the 17 GHz peak flux (70 to 4500 s.f.u.;

1 s.f.u. = 10^{-22} W m^{-2} Hz^{-1}) and the 50 keV peak flux (0.3 to 30 photons per s^{-1} cm^{-2} keV^{-1}).

In order to find the energy of the X-rays whose time evolution is most similar to the 17 GHz time evolution, we plot the 17 GHz flux versus the hard X-ray counting rates in a full logarithmic scale separately for each of the seven different energy channels. An example is shown in Figures 1(a) and 1(b). In the rising phase, the locus in the 17 GHz versus hard X-ray plane is invariably almost straight for all 22 flares, and thus we can safely assume that both hard X-rays and microwaves represent the common acceler-

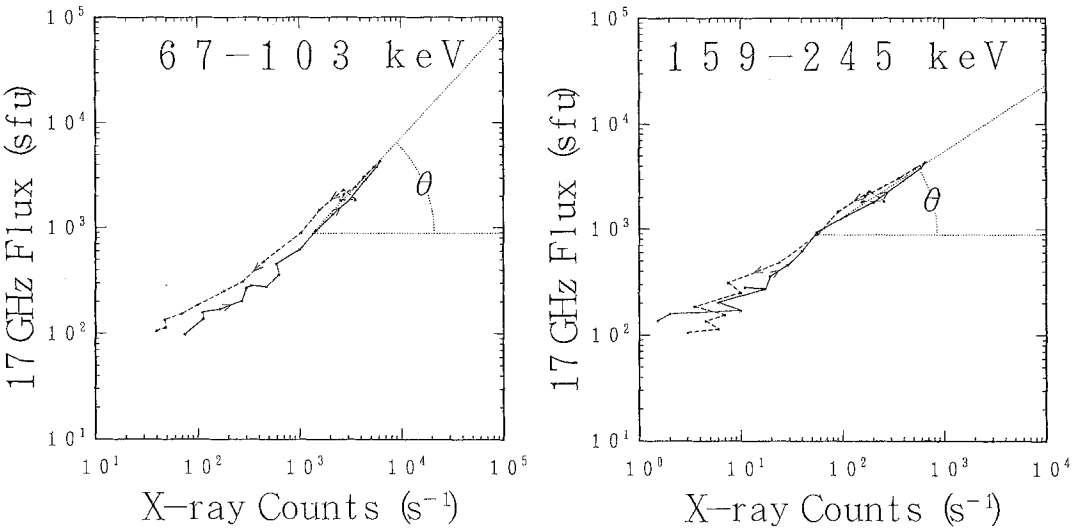

Fig. 1(a–b). Plots of the 17 GHz flux vs X-ray counting rates (background subtracted) with 2 s integration time for the burst of 15 October, 1981. The energy of the hard X-rays is shown in each plot. The data points in the rising phase are connected by solid lines, and those after the peak by dashed lines. Arrows indicate the time sequence. The logarithmic scale is equal for both quantities. θ is defined as the slope of the line connecting the peak and the onset ($\frac{1}{5}$ level and the peak of the 17 GHz flux).

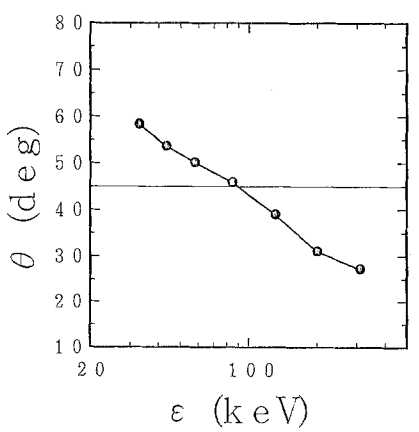

Fig. 1(c). Plots of θ with respect to the photon energy ε. The horizontal line is $\theta = 45°$.

ation/injection of electrons. On the other hand, there is an apparent microwave excess after the peak in 13 flares, although the present example does not belong to such flares. Therefore, we concentrate only on the rising phase during which the locus is straight, because in the declining phase the assumption of the same electron population for both microwaves and hard X-rays may not be valid.

The slope of the locus from the onset to the main peak of the burst in the full logarithmic plot is parametrized as θ, as indicated in Figures 1(a) and 1(b), i.e., $\tan\theta = \Delta\log(17\text{ GHz flux})/\Delta\log(\text{hard X-ray flux})$, so that θ is a measure of the ratio between the rise times of the 17 GHz flux and the hard X-ray flux; we prefer using θ instead of the ratio of rise times, because the latter is difficult to define for a multi-spike burst. Here, we rather arbitrarily take the time at which the 17 GHz flux is 1/5 of its peak value as the onset time. Plotting θ against the photon energy ε, we obtain a curve, as shown in Figure 1(c). Since the hard X-ray spectrum becomes harder during the rising phase, θ is a decreasing function of the photon energy ε. This tendency is also seen in Figure 2, where curves of θ vs ε for all the 22 flares are shown. Note that none of the flares show systematic spectral softening as time goes, as reported by Hoyng *et al.* (1976). For a flare in which the poor counting statistics make the uncertainty in the measurement of θ greater than 5° for higher-energy channels, we do not extend the curve to such channels.

These curves intersect with the line $\theta = 45°$ at a certain value ($\tilde{\varepsilon}$) of the photon energy. When a curve does not intersect with $\theta = 45°$ within the energy range covered by HXM (in 2 events), $\tilde{\varepsilon}$ is estimated from the extrapolation of the curve. The flux of X-rays measured at ε varies proportionally with the 17 GHz flux. Therefore we consider that the mean energy of electrons emitting photons of $\tilde{\varepsilon}$ is close to that of the microwave-emitting electrons. This interpretation is indirectly substantiated by the observed correlation between $\tilde{\varepsilon}$ and the X-ray power-law index at the peak determined from the 38–103 keV spectral observations (Figure 3). The general anticorrelation between the two quantities shows that the mean energy of microwave-emitting electrons is smaller for a softer electron spectrum, as expected. From this figure we find that $\tilde{\varepsilon}$ is below 100 keV for all but 5 of the events and that the median value of $\tilde{\varepsilon}$ is ~ 70 keV.

3. Energy of Microwave-Emitting Electrons

We demonstrate below that the energy of electrons emitting photons of energy $\tilde{\varepsilon}$ is close to that of electrons emitting microwaves. The tendency that θ decreases with ε, as seen in Figure 2 for *all* the flares, can be consistently explained by the hardening of the electron spectrum during the rising phase of a flare. Indeed, the X-ray spectrum shows a hardening from the onset to the peak (e.g., for the event in Figure 1, $\gamma = 2.9 \rightarrow 2.4$) and, therefore, the electron spectrum is expected to harden; the number of higher-energy electrons increases with time more rapidly than the number of the lower-energy electrons. Let us denote the mean energy of 17 GHz microwave-emitting electrons as $\overline{E_\mu}$ and that of electrons emitting X-ray photons with energy $\tilde{\varepsilon}$ as $\overline{E_X}$. Then if

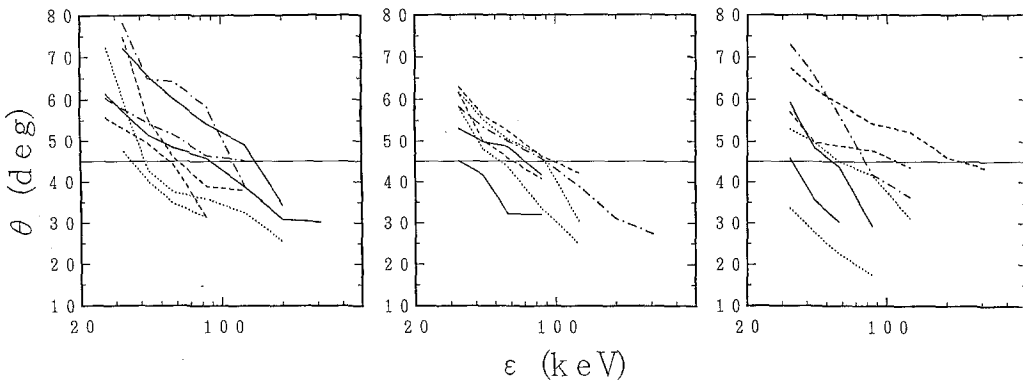

Fig. 2. θ vs ε curve for all 22 events.

$\overline{E_\mu} > (<) \overline{E_X}$, the rate of increase of the 17 GHz flux would be greater (smaller) than that of X-ray flux at $\tilde{\varepsilon}$, contrary to the observation.

Next we estimate quantitatively the energy range of electrons emitting photons of energy $\tilde{\varepsilon}$. This depends on the hard X-ray emission model: thin-target or thick-target. We calculate the relative contribution to the hard X-ray emission from electrons with a kinetic energy less than E keV, $\eta(E)$. Denoting the X-ray flux of photons with energy ε emitted by electrons with energy less than E as $I_\varepsilon(E)$, then we have

$$\eta(E) = \frac{I_{\tilde{\varepsilon}}(E)}{I_{\tilde{\varepsilon}}(\infty)} . \tag{1}$$

$I_\varepsilon(E)$ is different for thin-target and thick-target emissions. For thin-target emission,

$$I_{\tilde{\varepsilon}}(E) \sim \int_{\tilde{\varepsilon}}^{E} \frac{\mathrm{d}N(E')}{\mathrm{d}E'} E'^{1/2} Q_{\tilde{\varepsilon}}(E')\, \mathrm{d}E' , \tag{2}$$

where $\mathrm{d}N(E)/\mathrm{d}E$ is the instantaneous electron spectrum in the hard X-ray source, and $Q_\varepsilon(E)$ is the differential cross-section; here we use the Bethe–Heitler formula (Brown, 1971)

$$Q_{\tilde{\varepsilon}}(E) \sim \frac{1}{\tilde{\varepsilon}E} \log \frac{1 + \sqrt{1 - \tilde{\varepsilon}/E}}{1 - \sqrt{1 - \tilde{\varepsilon}/E}} . \tag{3}$$

When $\mathrm{d}N/\mathrm{d}E \sim E^{-\delta_{\mathrm{thin}}}$, $\delta_{\mathrm{thin}} = \gamma - 0.5$, where γ is the photon power-law index (Brown, 1971). For thick-target emission,

$$I_{\tilde{\varepsilon}}(E) \sim \int_{\tilde{\varepsilon}}^{E} \frac{\mathrm{d}^2 N(E_0, t)}{\mathrm{d}E_0\, \mathrm{d}t} \left[\int_{\tilde{\varepsilon}}^{E_0} E Q_{\tilde{\varepsilon}}(E')\mathrm{d}E' \right] \mathrm{d}E_0 , \tag{4}$$

where $\mathrm{d}^2 N(E_0, t)/\mathrm{d}E_0\, \mathrm{d}t\, (\sim E_0^{-\delta_{\mathrm{thick}}})$ is the flux of electrons injecting into the hard X-ray source region, and $\delta_{\mathrm{thick}} = \gamma + 1$ (Brown, 1971).

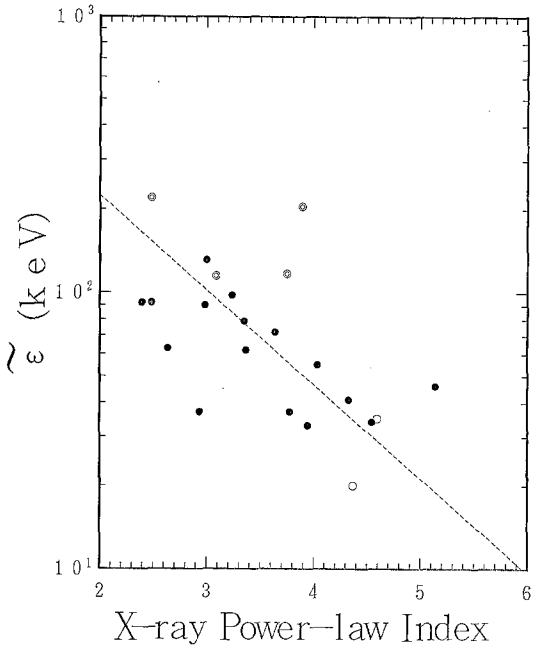

Fig. 3. Correlation between the photon energy $\tilde{\varepsilon}$ at which the X-rays vary at the same rate as the 17 GHz flux ($\theta = 45°$) and the X-ray power-law index γ_{peak} between 38 and 103 keV at the peak. Events represented by double circles and open circles correspond to the exceptional events in Section 4.

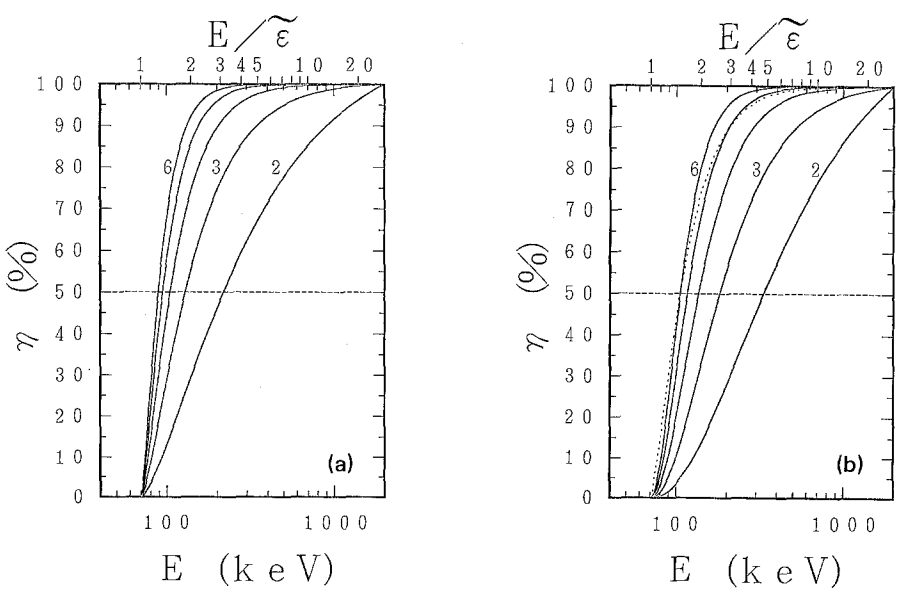

Fig. 4. Relative contribution to the 70 keV X-rays from the electrons with a kinetic energy less than E keV for the thin-target case (a) and the thick-target case (b). Each curve, from right to left, corresponds to the different photon power-law indices of $\gamma = 2$, 3, 4, 5, and 6, of which only 2, 3, and 6 are displayed. These curves are scaled with $E/\tilde{\varepsilon}$ as indicated on the upper axis. In (b), the curve for $\gamma = 4$ in the thin-target case is reproduced (dotted line) for comparison.

We depict $\eta(E)$ for X-rays with energy $\tilde{\varepsilon} = 70$ keV (the median value in Figure 3) in Figure 4(a) for the thin-target case and in Figure 4(b) for the thick-target case. In these figures each curve corresponds to a different photon power-law index. This result can be scaled with $E/\tilde{\varepsilon}$; i.e., $\eta(E)$ is taken as a function of $E/\tilde{\varepsilon}$. We define the mean energy ($\overline{E_X}$) of electrons emitting photons of $\tilde{\varepsilon}$ as the energy where $\eta = 50\%$. This depends on the hard X-ray spectrum as shown in these figures. For $\gamma = 5$ to 3, in which most events lie (Figure 3), $\overline{E_X} = 1.4$–$1.8\ \tilde{\varepsilon}$ for the thin-target case, and $\overline{E_X} = 1.7$–$2.6\ \tilde{\varepsilon}$ for the thick-target case. Therefore, $\tilde{\varepsilon} = 70$ keV corresponds to $\overline{E_X} = 100$–130 keV (thin-target), and $\overline{E_X} = 120$–180 keV (thick-target). Thus, we conclude that the energy of microwave-emitting electrons is at most a few hundred keV for most of the flares.

4. Model of Hard X-Ray and Microwave Sources

The θ vs $\tilde{\varepsilon}$ curve or $\tilde{\varepsilon}$ presented in Section 2 depends on both the hard X-ray emission model (thin-target and thick-target) and the magnetic field strength (B) in the microwave source. Therefore, it is possible to determine them by fitting the calculated θ vs ε curve to the observed curve.

Models we consider are a thin-target and a thick-target model. In the thin-target case, both hard X-rays and microwaves are thought to be emitted by electrons trapped in the corona, where the ambient ion density is n_0. Since the electron spectrum deduced from the hard X-ray spectrum is proportional to n_0^{-1} (Brown, 1971), the calculated microwave flux is also proportional to it. In the thick-target model we assume that both hard X-rays and microwaves are emitted by electrons precipitating from the corona (Kai *et al.*, 1985; Kai, 1986); X-rays in regions of extremely high density, and the 17 GHz emission in regions slightly above, where the local plasma frequency is lower than 17 GHz. The microwave flux depends on the instantaneous number of electrons contained within the microwave source. This number can be derived from the electron flux $\mathrm{d}^2N/\mathrm{d}E\ \mathrm{d}t$, which is calculated from the hard X-ray spectrum (Brown, 1971), multiplied by a time δt during which the precipitating electrons pass through the radio source. We have $\delta t = L/v_\parallel$, where L is the vertical length of the radio source and $v_\parallel$ the velocity component parallel to the magnetic field lines of force. Since $v_\parallel$ is related to E by $v_\parallel^2 = v^2/3 = c^2(\gamma^2 - 1)/3\gamma^2$ and $\gamma = 1 + E/mc^2$, where c is the light velocity and m the electron mass, or by $v_\parallel^2 = 2E/3m$, for $\gamma - 1 \ll 1$ (non-relativistic case), L is the only unknown parameter.

In order to obtain the θ vs ε curve, we calculate the 17 GHz flux at both the onset and the peak with the same (arbitrary) L and n_0. The electron spectra are derived from the observed hard X-ray spectra (fitted to a single power-law) with use of the formula by Hudson *et al.* (1978). In calculation of gyrosynchrotron emission, we use the formula given by Melrose (1980), assuming that

(1) the microwave source is optically thin;
(2) the pitch angle distribution is isotropic;
(3) the low- and high-energy cutoffs are 20 keV and 2 MeV, respectively;
(4) the magnetic field is uniform; and
(5) the line-of-sight makes an angle of 45° with respect to the magnetic field.

For the same example as illustrated in Figure 1, the calculated θ vs ε curves are shown for both the thick-target and thin-target cases (Figure 5(a)) with various magnetic strengths B. We plot in Figure 5(b) the calculated $\tilde{\varepsilon}$ against B to compare with the observations. The magnetic field strength for which the calculated $\tilde{\varepsilon}$ fits to the observed $\tilde{\varepsilon}$ is larger for the thin-target case (1800 G) than for the thick-target case (850 G). This

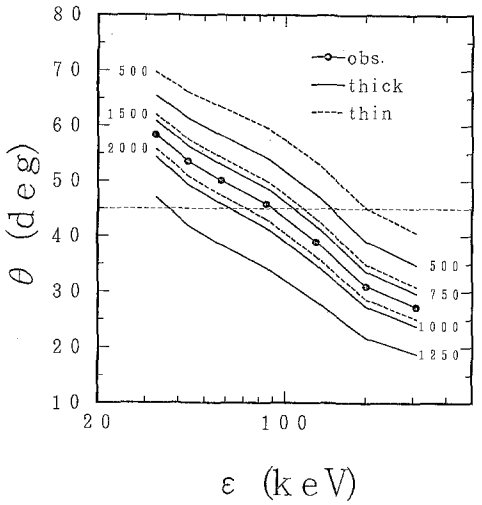

Fig. 5(a). Calculated θ vs ε curve of the 15 October, 1981 flare, shown in Figure 1, for various magnetic field strengths B for the thick-target (solid lines) and thin-target (dashed lines) cases. The observed θ vs ε curve is reproduced for comparison.

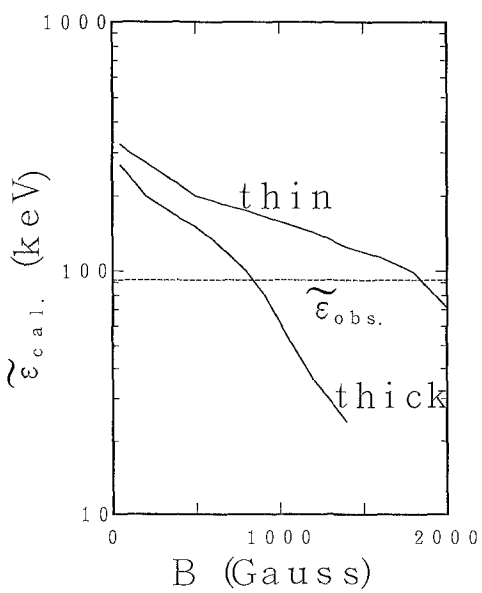

Fig. 5(b). The calculated photon energy at which $\theta = 45°$ is plotted as a function of the magnetic field strength B for both cases. The observed $\tilde{\varepsilon}$ (= 92 keV) is shown in a dashed line.

is understood as follows. Since the electron spectrum deduced from the observed hard X-ray spectrum on the assumption of the thick-target model is softer than that deduced on the thin-target assumption, the mean energy of microwave-emitting electrons would be lower in the thick-target case, if the field strength were the same. However, from Figure 4(b), we are confronted with the opposite result; e.g., for an X-ray spectrum with a power-law index $\gamma = 4$, $\overline{E_\mu}$ is $1.5\tilde{\varepsilon}$ for the thin-target case, and $2.0\tilde{\varepsilon}$ for the thick-tarhet case; i.e., $\overline{E_\mu}$(thick-target) > $\overline{E_\mu}$(thin-target). Thus, to make the effective energy lower in the thin-target case, a stronger magnetic field is required. Note that the estimation of B depends on neither L nor n_0 as long as they do not change with time, because, in calculating the θ vs ε curve, we need only the ratio of the 17 GHz fluxes at two times.

Next, in order to test which model is more likely, we estimate L for the thick-target case and n_0 for the thin-target case using B obtained above, from the comparison of the calculated 17 GHz flux with the observed one. Then for the flare shown in Figure 5, $L \sim 9 \times 10^3$ km and $n_0 \sim 2 \times 10^{14}$ cm^{-3}. The value of L is not unlikely, considering that the observed source size is generally $\sim 10''$ (Alissandrakis and Kundu, 1978; Marsh and Hurford, 1980; Kosugi *et al.*, 1983). On the other hand, the value of n_0 is so large that the thin-target assumption is no longer valid. Thus, we conclude that at least for the example in Figure 5 the thick-target case (B = 850 G) is more likely than the thin-target case (B = 1800 G). As a check of the assumption of optically-thin radio emission, identically, we have calculated the optical thickness at 17 GHz due to the self-absorption, using the above values of L or n_0 for assumed circular source area of $10''$ in diameter. In both the thick-target and thin-target cases, the optical thickness of the source < 1. For the remaining 21 flares, we obtain B for which the calculated $\tilde{\varepsilon}$ is equal to the observed $\tilde{\varepsilon}$, just in the same way as illustrated above. These flares show that B(thin-target)/B(thick-target) = 1.6–2.2. Figure 6 displays the distribution of B

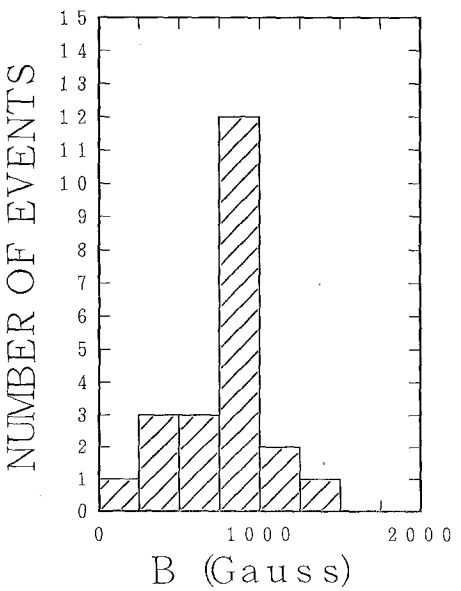

Fig. 6. Distribution of the magnetic field strength determined from the thick-target model for the 22 events.

obtained on the assumption of the *thick-target* model for the 22 flares. We obtain $B \geqq 500$ G for 18 events, in which all but two have L of between 2 and 25×10^3 km, and 15 have L of less than 10×10^3 km. Since the microwave flux is very sensitive to B, the possible error, even though small, in estimating B will cause a factor-of-two uncertainty in L. Thus the above values of L is compatible with the observed source size of $\sim 10''$ (Alissandrakis and Kundu, 1978; Marsh and Hurford, 1980; Kosugi *et al.*, 1983). On the other hand, n_0 derived on the thin-target assumption is $\gtrsim 2 \times 10^{13}$ cm^{-3}. Therefore, we conclude that 16 flares out of 22 can be explained by the thick-target model. Incidentally, in Figure 3, where the anticorrelation between $\tilde{\varepsilon}$ and the X-ray power-law index at the peak is shown, the flares for which L does not fall in the reasonable range are distinguished from the 16 flares; the 2 events for which L is too small are represented as open circles and the 4 events for which L is to large (corresponding to $B < 500$ G) as double circles.

Once B is known, we can calculate the energy range of electrons contributing to the 17 GHz flux. If the effective energy of electrons for the 17 GHz emission is close to that of electrons emitting photons of $\tilde{\varepsilon}$, our method proves to be self-consistent. For the example illustrated in Figure 5 (the event having the hardest spectrum), we have calculated the relative contribution to the 17 GHz flux from electrons with energy below E keV, using the known value of B. Figure 7 shows, for the thick-target case, the comparison of the contribution curves to the 17 GHz flux with that to the X-rays of $\tilde{\varepsilon}$. We find that energy at which η is 50% is nearly the same in both cases, although the contribution function for the 17 GHz emission is somewhat broader than that for X-ray

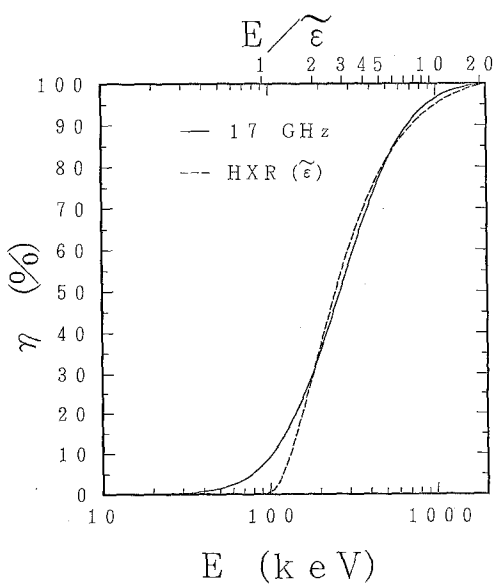

Fig. 7. Relative contribution to the 17 GHz flux from the electrons with a kinetic energy $< E$ keV calculated for the event of Figure 1. Contribution curve for the X-rays of an energy $\tilde{\varepsilon}$ is also shown in comparison (dashed line).

emission. Consequently, we conclude that our method of deducing the energy of microwave-emitting electrons and the magnetic field strength from the observed $\tilde{\varepsilon}$ proves to be self-consistent. It is to be noted that, for this flare, because of the large $\tilde{\varepsilon}$ (92 keV) and the hard spectrum ($\gamma = 2.4$), the mean energy of electrons responsible for the 17 GHz emission is rather high (~ 240 keV); it is lower for other events.

5. Discussion

We have compared the rate of increase of the 17 GHz microwave flux with that of the hard X-ray flux in different energy channels from the onset to the peak for the selected 22 flares. From the energy $\tilde{\varepsilon}$ of X-rays which increase proportionally with the 17 GHz flux, we have estimated the mean energy of electrons contributing to the 17 GHz emission is below a few hundred keV. This immediately leads us to expect a strong magnetic field, and hence a low altitude of the microwave source. Indeed, by calculating the rate of increase of the 17 GHz flux relative to that of the hard X-ray flux for a number of values of magnetic field strength and comparing the calculated rate of increase with the observed one, we have obtained, for the majority of flares, a magnetic field of 500–1000 G for the thin-target case. Further, from the comparison of the 17 GHz flux calculated with the obtained B with the observed flux, we have concluded that only the thick-target case is likely; a length of the microwave source in the range $2–25 \times 10^3$ km is required in the thick-target case, while the ion density of more than 2×10^{13} cm^{-3} is required in the thin-target case, which is too large for the thin-target assumption. As we confine ourselves to relatively intense events, we claim that our numerical results are without much error.

We discuss below whether the assumptions made in using the θ vs ε curve or $\tilde{\varepsilon}$ to derive the energy of microwave-emittion electrons and the magnetic field strength are relevant. We have assumed that the observed θ vs ε curve is free from the saturation of microwaves due to the self-absorption. Now, suppose the case in which the optical thickness of the microwave emission increases during the rising phase and exceeds unity at the peak. Since the saturation makes the rate of the increase of the microwave flux smaller, the θ vs ε curve is observed to be below that which would be observed when no saturation occurs. Thus, we are led to underestimate $\tilde{\varepsilon}$ or $\overline{E_\mu}$ and, hence, overestimate B. However, the observed 9.4 GHz flux (*Monthly Report of Solar Radio Emission*, Toyokawa Observatory) is larger than the 17 GHz flux in 19 flares out of 22. Therefore, we conclude that the saturation does not seriously affect the result. Next, we consider the change in B. If B increases (decreases) from the onset to the peak, the microwave flux increases more (less) rapidly than does in the constant B. Therefore, the increase (decrease) in B during the rising phase results in overestimating (underestimating) $\tilde{\varepsilon}$. Consequently, if the observed θ vs ε curve is affected seriously by the change in B, the anticorrelation between $\tilde{\varepsilon}$ and the X-ray power-law index at the peak would be greatly scattered. However, Figure 3 shows that such an effect, if any, is not large.

Next, let us compare our results with the recent work by Gary (1985), who has shown

that observed microwave and hard X-ray fluxes can consistently be explained if thick-target emission and a magnetic field strength of 300 G are assumed. The difference in B between his (300 G, an assumed value) and ours (500–1000 G) naturally causes the difference in the number of electrons needed for microwave emission; in our calculation in the thick-target case, $N(> 20\ \text{keV})$ is in the range $1\text{–}15 \times 10^{34}$, which, even if we extrapolate the low-energy end to 10 keV, is at least an order of magnitude less than $N(> 10\ \text{keV})$ of Gary. Such a difference in B arises mainly from the different assumptions regarding the dependence of δt on E; δt is independent of E in the Gary's treatment, while it becomes proportional to $E^{-1/2}$ for non-relativistic energies in the present study. For B of ~ 300 G, the mean energy of microwave-emitting electrons would be ~ 1 MeV, the corresponding $\tilde{\varepsilon}$ being ~ 500 keV, much higher than the values ($\lesssim 100$ keV) obtained here. Moreover, our results are in agreement with the good correlation found between the peak 17 GHz flux and the peak 70–150 keV X-ray flux (Kai *et al.*, 1985).

Of the 22 events studied here, 16 can be successfully explained by the thick-target model. However, there are 6 events which cannot consistently be explained by the thick-target model. Of these, 2 events (shown in Figure 3 as open circles) give $L \lesssim 3 \times 10^2$ km and show small $\tilde{\varepsilon}$ and a stronger (> 1000 G) magnetic field. The microwave emission from these flares is probably of thermal origin. The hard X-ray spectrum is soft ($\gamma > 4.3$), and the flux varies relatively gradually. Four of the six events for which L was calculated to be $> 8 \times 10^4$ km (represented as double circles in Figure 3) show relatively large $\tilde{\varepsilon}$, and the calculated magnetic field is weak (< 500 G). The thin-target model still gives an unreasonably large value of $n_0 \gtrsim 10^{12}\ \text{cm}^{-3}$ for these 4 events. For these events we may not be able to assume that a common electron population is responsible for the hard X-rays and microwaves.

Acknowledgements

We would like to express our deepest thanks to the members of the Hinotori team of the Institute of Space and Astronautical Sciences for design and construction of the Hard X-Ray Monitor Spectrometer. We are also grateful to Dr K. Kai for useful suggestions during the course of this work. Dr B. R. Dennis is particularly acknowledged for the critical reading of the manuscript.

References

Alissandrakis, C. E. and Kundu, M. R.: 1978, *Astrophys. J.* **222**, 342.
Brown, J. C.: 1971, *Solar Phys.* **18**, 489.
Cornell, M. E., Hurford, G. J., Kiplinger, A. L., and Dennis, B. R.: 1984, *Astrophys. J.* **279**, 875.
Crannell, C. J., Frost, K. J., Mätzler, C., Ohki, K., and Saba, J. L.: 1978, *Astrophys. J.* **223**, 620.
Gary, D: E.: 1985, *Astrophys. J.* **297**, 799.
Holt, S. and Ramaty, R.: 1969, *Solar Phys.* **8**, 119.
Holt, S. and Cline, R.: 1968, *Astrophys. J.* **154**, 1027.
Hoyng, P., Brown, J. C., van Beek, H. F.: 1976, *Solar Phys.* **48**, 197.
Hudson, H. S., Canfield, R. C., and Kane, S. R.: 1978, *Solar Phys.* **60**, 137.

Kai, K.: 1986, *Solar Phys.*, in press.
Kai, K., Kosugi, T., and Nitta, N.: 1985, *Publ. Astron. Soc. Japan* **37**, 155.
Kane, S. R.: 1974, in G. Newkirk, Jr. (ed.), 'Coronal Disturbances', *IAU Symp.* **57**, 105.
Kane, S. R. and Anderson, K. A.: 1970, *Astrophys. J.* **162**, 1003.
Kane, S. R., Crannell, C. J., Datlowe, D. W., Feldman, U., Gabriel, A., Hudson, H. S., Kundu, M. R., Mätzler, C., Neidig, D., Petrosian, V., and Sheeley, N. R., Jr.: 1980, in P. Sturrock (ed.), *Solar Flares*, Colorado Associated University Press, Boulder, p. 187.
Kosugi, T., Kai, K., and Suzuki, T.: 1983, *Solar Phys.* **87**, 373.
Marsh, K. A. and Hurford, G. J.: 1980, *Astrophys. J.* **240**, L111.
Melrose, D. B.: 1980, *Plasma Astrophysics*, Gordon and Breach, New York.
Nitta, N.: 1984, 'X-Ray Continuum Spectra in Solar Flares', Thesis, University of Tokyo, Tokyo.
Ohki, K., Nitta, N., Tsuneta, S., Kakakura, T., Makishima, K., Murakami, T., Ogawara, Y., and Oda, M.: 1982, in *Hinotori Symposium on Solar Flares*, ISAS, Tokyo, p. 69.
Takakura, T.: 1972, *Solar Phys.* **26**, 434.